An Intelligent Model and Simulation of High Voltage and Medium Voltage Transmission Line Protection Scheme Using Time Overcurrent Relay Optimization Settings

Boniface Ntambara (bonifacen@ieee.org)
Moi University https://orcid.org/0000-0001-9915-5421
Simiyu Stanley Sitati
Moi University
Paul M. Wambua
Moi University
Byiringiro Jean Bosco
Dedan Kimathi University of Technology

Research Article

Keywords: High Voltage Transmission line, Overcurrent Relay Setting, Power System Protection, MATLAB/Simulink 2019a, OCR characteristics

Posted Date: December 28th, 2023

DOI: https://doi.org/10.21203/rs.3.rs-3813605/v1

Additional Declarations: The authors declare no competing interests.

An Intelligent Model and Simulation of High Voltage and Medium Voltage Transmission Line Protection Scheme Using Time Overcurrent Relay Optimization Settings

Boniface Ntambara, *Member, IEEE*, Simiyu Stanley Sitati, Paul M. Wambua, and Jean Bosco Byiringiro

***Abstract*—A new method for optimizing overcurrent relay (OCR) settings and coordination in interconnected power systems was developed. The method considers factors such as feeder impedance equivalences, phase-to-phase fault currents, current settings of 110kV incoming and 15kV outgoing feeders, and operating times for relay characteristics (standard, very, and extremely inverse of overcurrent relay). The maximum fault current of the interconnected power grids is also considered. Power system parameters like X/R ratio, current transformer ratio, transmission line length, resistances, inductances, full load current, line capacity, CT ratio for outgoing feeders, grid frequency, and real power are also considered. To ensure safety and rapid operation of overcurrent relays, settings such as pickup value, time setting multiplier (TMS), and OCR characteristics are carefully considered. The results show that the OCRs coordination interval time to fastest clear faults range from 0.0927 sec-0.062 sec to 0.0764 sec-0.0661 sec for extremely, very, and standard inverse relays, respectively.**

***Index Terms*— High Voltage Transmission line, Overcurrent Relay Setting, Power System Protection, MATLAB/Simulink 2019a, OCR characteristics.**

I. Introduction

Medium and high-voltage transmission pathways are widely used for transferring energy from production to delivery, specifically designed for high-voltage levels like 70kV, 110kV, 132kV, 220kV, and 500kV, to reduce inefficiencies in large-scale electricity conveyance [1]. The OCR inverse-time characteristic is useful in electric-utility distribution-circuit security due to its ability to regulate incident-current amplitude, which is largely determined by fault position and unregulated by fluctuations in generating units or high-voltage transmission infrastructure. Relays with extremely reversing profiles are suitable for this purpose, but their inverse aspect may not be beneficial if the magnitude of grounded-fault current is significantly constrained by neutral-grounding impedance [2]. Timely inverse OCRs have both immediate and time-delay components on an identical module. Initially, electromechanical relays were used for overcurrent protection. The most sophisticated microcomputer defense includes three separate phases overcurrent and earth-fault units. Configuring OCRs with the requisite time/current characteristics is crucial for optimal performance [3]. These types of relays are usually linked to potential transformers and regulated to work on, either above or below an appropriate voltage or current level [4]. Relay coordination is critical in the defense response. As part of the overall system protection, it is necessary to identify and isolate the faulty circuit only, prohibiting the tripping of the healthy circuits [5]. For a safe and secure protection strategy, if the principal protective system is unsuccessful, a reliable backup ought to be present and redundant defense must function as a fallback alternative either in the identical power station or in adjacent lines with a time interval based on the requirements [6]. Electricity networks are essential parts of the power grid due to they serve as an interface for electricity to be transferred from the energy source to the load via transmission lines which operate at dissemination voltages that are that vary between 15 kV to 110 kV as well as are intended to be securely complemented for reliable execution; however, line failures frequently disrupt the supply of electricity and influence the whole power system, resulting in severe blackouts [7]. The transmission line networks were responsible for almost 2/3 of the power system's problems [8]. High-medium voltage line security plays an important role in power system dependability by sensing the existence of an interruption on the transmission network and promptly sending the signal in order to trigger the protective devices at both ends and separate the hazardous section [9].

II. Review of Related Works

Transmission network defense has been achieved using distance protection approaches, but these have limitations like sensitivity to fault resistance and infeed current from remote sources. A pilot wire inverted overcurrent relay protection scheme is preferred due to its high sensitivity, selectivity, and speed of operation. This technology improves operating speed and can provide beneficial performance during power fluctuations and external failures. [10]**.** In, a Time-frequency Analysis-Based Relay Protection Method for High Voltage Transmission Lines was developed in [11]. Based on time-frequency analysis, the failure signal of the high-voltage transmission line was retrieved. Decomposing the fault signal characteristics detects the fault transient component of a high-voltage transmission line. The relay protection of the high voltage power transmission line is realized using phase correlation protection based on the fault transient component. This proposed system was 100%

Boniface Ntambara is with Department of Manufacturing, Industrial, and Textile Engineering, Moi University, P.O BOX 30900-3100 Eldoret, KENYA bonifacen@ieee.org .
Simiyu Stanley Sitati is with Department of Electrical and Telecommunication Engineering, Moi University, P.O BOX 30900-3100Eldoret, KENYA. Email: simiyusitati@yahoo.com.
Jean Bosco Byiringiro is with Department of Mechatronics and Automation Engineering, Dedan Kimathi University of Technology, P.O BOX 2100 Nyeri, KENYA. Email: jeanbosco@dekut.ac.ke .
Paul M. Wambua is with Department of Mechanical, Production and Energy Engineering, Moi University
P.O BOX 30900-3100Eldoret, KENYA. Email: Paulwambua@yahoo.com

effective, demonstrating the method's dependability; nonetheless, the protective system's speed and selectivity were inadequate. In, a new high-voltage transmission line protection method based on traveling wave energy comparison was devised and developed [12]. The high frequency band energy of voltage travelling waves is determined using the S-transform, and protection judgment is built using the ratio of backward and forward travelling wave energy on the same side of the transmission line. The energy ratio near the fault is less than one, while the farthest away side has more than one for the external fault. Both sides of the internal fault have more than one energy ratio. The proposed method is adaptable, fast, and reliable when using PSCAD/EMTDC for simulation verification. A protection of high voltage transmission lines connected to large-scale wind farms was also developed in [13]. The nonlinear wind speed and power characteristics of turbine generators (TGs), complex control actions, and low voltage ride-through capabilities significantly affected transmission line impedance during fault and normal situations. TGs were integrated into the main utility grid, generating electricity via high voltage long transmission lines. It was proposed to use protection relays routinely used to protect transmission lines in a differential relay power protection system. Changes in the proportion of observed current and voltage from the configuration side to the fault detection point are noticed and responded to by these relays. [14]. The basic distance defensive relaying approach is intended to figure out the susceptibility measurement for the fault line employing both the current and voltage of the shielding side and then contrast it to the configuration line obstruction to determine a fault situation [15]. To change the phase distance relays, the positive-phase sequence impedance between the relay site and the fault location beyond which the operation of a specific relay unit should stop was used in order to secure the transmission line units [16]. The study addresses research gaps on transmission line protection techniques and their disadvantages, resulting in power outages. It reveals that these systems are not proportionate to fault occurrences, display inadequate action speed, and unreliability of relaying requirements, causing power network performance issues and major blackouts. The study proposes time inverse overcurrent relay setting characteristics to meet quick relaying system requirements during power outages and fault locating.

III. MATERIALS AND METHODS

A new method for optimal overcurrent relay settings and coordination in interconnected power systems has been developed. The method considers factors such as feeder impedance equivalences, phase to phase fault currents, current settings of 110kV incoming and 15kV outgoing feeders, and operating times for relay characteristics. The maximum fault current of the grids is recorded and documented. The network MVA short circuit is considered with both positive and negative sequence impedance of the feeder. Power system parameters like X/R ratio, CT ratio, transmission line length, resistances, inductances, full load current, line capacity, current transformer ratio, grid frequency, and real power are considered. To ensure safe, reliable, and rapid operation of overcurrent relays, settings such as pickup value, time setting multiplier (TMS), and overcurrent relay (OCR) characteristics are carefully considered. Fig. 1 shows the steps that were followed in the pickup value selection of the overcurrent relay.

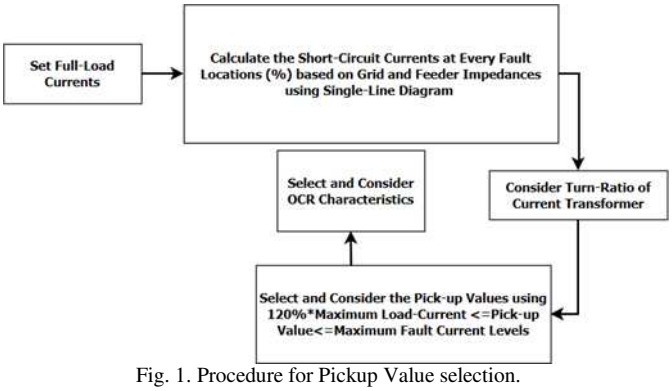

Fig. 1. Procedure for Pickup Value selection.

Fig. 2 demonstrates the single line schematic of substation with transformer 110/15 kV, 10 mega volt-ampere (MVA), distributed feeders F1, F2, F3, F4 and Spare F5 for a considered fault location of 0%, 1%, 25%, 50%, 75%, and 100%.

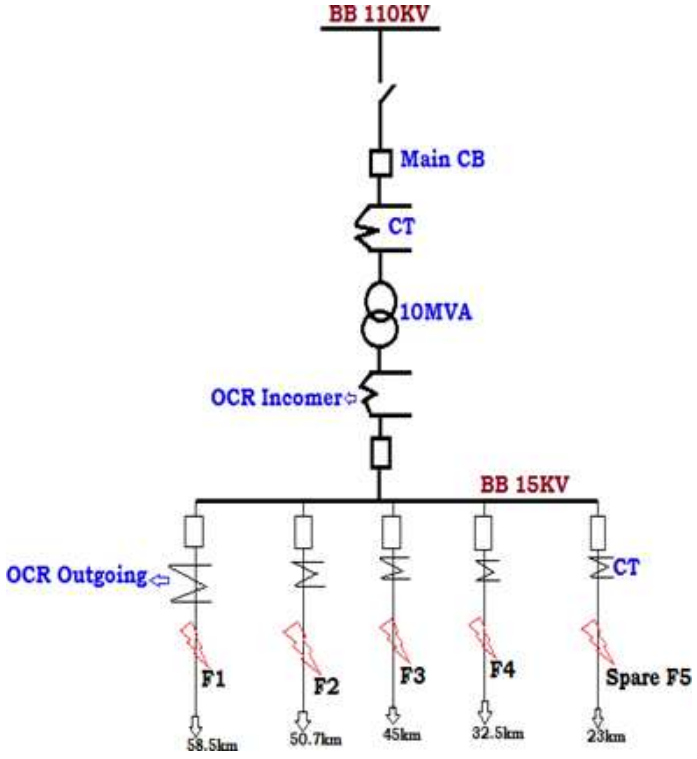

Fig. 2. Incoming and outgoing (Feeders) of overcurrent relay

MATLAB/Simulink 2019a software was used to model and test the power system protective relaying. Table 1 shows the parameter and setting values used to develop and test the Rwanda power network as described in this paper.

Table 1. Power Network Setting Parameters.

S/N	Parameters and descriptions	Values
1.	($Z_1 = Z_2$) positive and negative sequence impedance	0.045+j 0.151 Ω/km
2.	Transmission line length	100Km
3.	Time setting Multiplier (TMS)	0.05sec
4.	positive and zero sequence resistances	0.04553 & 0.1517 in Ω/km
5.	positive and zero sequence inductances	0.000617 & 0.001533in H/km
6.	Line capacity	282MVA
7.	Incoming line voltage	110kV
8.	grid frequency	50Hz
9.	CT ratio for outgoing feeders	500/1A
10.	X/R ratio	5
11.	CT ratio	2500/4A
12.	Outgoing feeder voltage	15kV
13.	MVA short circuit	2587 MVAsc
14.	full load current	1840.9A
15.	real power	70MW

The data of grid impedance (X_{S110KV}), transformer impedance (X_t), and feeder impedance (X_f) at fault locations are required for the computation of Phase short circuit currents and were calculated in equations (1) to (2). The feeder impedance at the transformer and at the fault location considering the feeder distance is illustrated in Table 2.

Table 2. Feeder Impedance Calculations.

% Fault Location	Feeder Impedances in Ω/km
0	0%*58.5*(0.045 + j 0.151) = 0
1($\mathbf{X_{F1}}$)	1%*58.5*(0.045 + j 0.151) = 0.026+ j 0.088

$$X_{S\,110kV} = {(KV)^2}/{MVAsc} \quad (1)$$

$$X_{s110kV} = {(110)^2}/{2587} = \mathbf{4.677\ \Omega}$$

The grid impedance ($X_{f\,15KV}$) of 15kV outgoing (feeders)

$$X_{f\,15kV} = \frac{(X_{S15kV})^2}{(X_{S110kV})^2} * (X_{S110kV}) \quad (2)$$

By replacing the value of $X_{S15kV} = 15kV$ and $X_{S110kV} = 110kV$, into equation (2),

$$X_{f\,15kV} = \frac{15^2}{110^2} * 4.677\Omega = \mathbf{0.086\Omega}$$

The line impedance of incoming of incoming of the power grid and outgoing feeder were produced Fig. 3 indicates the equivalent transmission line impedance diagram reduced from equations (1) and (2) for the corresponding 110kV and 15kV sides respectively and equation (3) shows the transformer impedance (X_t) of power distribution outgoing side.

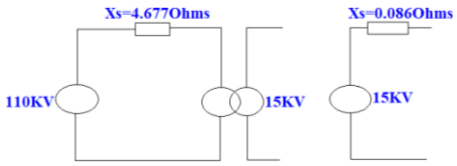

Fig. 3. Reference of Xs from bus-bar 15KV.

$$X_t = \frac{(kV)^2}{MVA} * 8.67\% \quad (3)$$

Where the 8.67% is the grid transformer performance

$$X_t = \frac{(15)^2}{10} * 8.67\% = 1.95\Omega.$$

The study analyzed the impact of feeder line impedance on short circuit current calculations, considering the length from the 15 kV bus-bar to the far end outgoing feeder fault location. The longest feeder, F1, was chosen for calculations due to its length of 58.5 km. The impedances were calculated at 0% of the fault location and 1% of F1's length. The network's negative and positive sequence resistances of ($Z_1 = Z_2 = 0.045 + j\,0.151$) in Ω/km was recorded and considered in this feeder impedance calculation as shown in table 2. The corresponding equivalent of feeder impedances regarding the fault location was also calculated in series and used to find the fault current levels in the network as demonstrated in equation (4) to (7).

$$Z_{eq} = F_{loc} * F.L * X_{FR} + Z_{FI} \quad (4)$$

$$Z_{1eq} = Z_{2eq} = X_{s(15KV)} + X_t + X_{F1} \quad (5)$$

$$Z_{1eq} = Z_{2eq} = 0.045 + j0.151 + X_{F1} \quad (6)$$

$$Z_{1eq} = Z_{2eq} = j0.086 + j1.95 + X_{F1} = j2.036 + X_{F1} \quad (7)$$

Where Z_{eq} is equivalence feeder impedance, F_{loc} is fault location (%), F. L is feeder length, X_{FR} is sequence feeder reactance (Ω/km), Z_{FI} is feeder impedance at 0%. This work focuses on setting relay settings and substation relay coordination parameters. Power network characteristics are set, including sequence resistances, high-medium voltages, current full-load, MVA and MVAsc, X/R and CT ratio, multiplier period, and system frequency. Fault level currents are calculated by matching feeder impedances to fault locations. The Operational Time Control (OCR) computes the plug setting multiplier for faulty power network component isolation. The actual operational time of the relay is calculated to configure OCR and coordinate with backup protection as shown in Fig. 4.

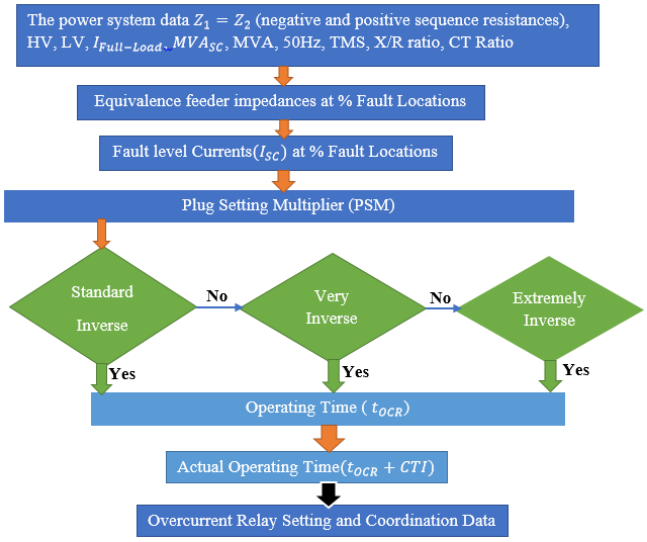

Fig. 4. The flowchart of overcurrent relay settings and relay coordination.

Based on short circuit currents at a 15 kV bus, the overcurrent relay operation time (t_{OCR}) and OCR coordination time were calculated. The regulated and controlled time multiplier setting (TMS = 0.05 sec) was studied and chosen based on overcurrent relay characteristics as given in equations (8) to (11) that represent the conventional inverse, very inverse, and extremely inverse of the relay.

$$\text{SI: } t_{OCR} = \frac{0.14}{Psm^{0.02}-1} * TMS \quad (8)$$

$$\text{VI: } t_{OCR} = \frac{13.5}{Psm-1} * TMS \quad (9)$$

$$\text{EI: } t_{OCR} = \frac{80}{Psm^{2}-1} * TMS \quad (10)$$

$$\text{Where} \qquad Psm = \frac{I_{SC}}{I_{set}} \quad (11)$$

SI: standard inverse of Relay, VI: Very inverse of the relay, EI: extremely inverse of the relay. By replacing equation (11) in equations (8), (9), and (10), the operating time of OCR characteristics were determined as shown in equations (12), (13), and (14).

- ✓ **Standard Inverse relay characteristics**

$$t_{OCR} = \frac{0.14}{(\frac{I_{SC}}{I_{set}})^{0.02}-1} * TMS \quad (12)$$

- ✓ **Very Inverse relay characteristics**

$$t_{OCR} = \frac{13.5}{(\frac{I_{SC}}{I_{set}})-1} * TMS \quad (13)$$

- ✓ **Extremely Inverse relay characteristics**

$$t_{OCR} = \frac{80}{(\frac{I_{SC}}{I_{set}})^{2}-1} * TMS \quad (14)$$

Where t_{OCR}: The overcurrent relay tripping time. The outgoing feeder used a current transformer ratio was 500/1A as illustrated in Fig. 5. The OCR feeder relay side's setting current (I_{set}) was 120% of the full load current ($I_{Full-Load}$) installed equipment (CT) of 500 A. The equation (15) shows the OCR feeder current setting used in computation of relay operating and coordination time.

$$I_{set} = 120\% * I_{Full-Load} \quad (15)$$

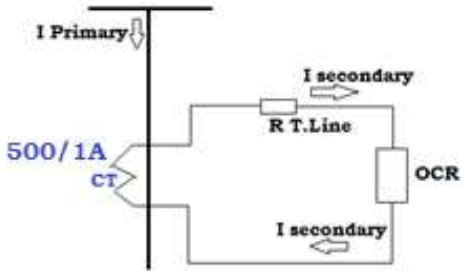

Fig. 5. Current Transformer Ratio.

The OCR incoming relay side's current setting (I_{set}) of 120% of the full load ($I_{Full-Load}$) equipment installed was chosen and designed to withstand severe loads. The lowest current ($I_{Full-load}$) of 1840.9 A of the installed transformer was considered. The equation (16) depicts the incoming current relay setting.

$$I_{set} = 120\% * I_{Full-Load} \quad (16)$$

The performance of overcurrent and auto-reclose relays before, during, and after fault circumstances has been assessed using sophisticated models of OCRs in power systems. The electrical system has been designed and tested. The overcurrent and auto-reclose relay logic models in this research were developed as subsystems, as shown in Figs. 6 and 7 respectively, and were then implemented in the power system, as shown in Fig. 8. The logic of auto-reclose and overcurrent relays was to send opening or closing signals to the relevant circuit breaker if the fault current exceeded or fell on installed equipment's set current.

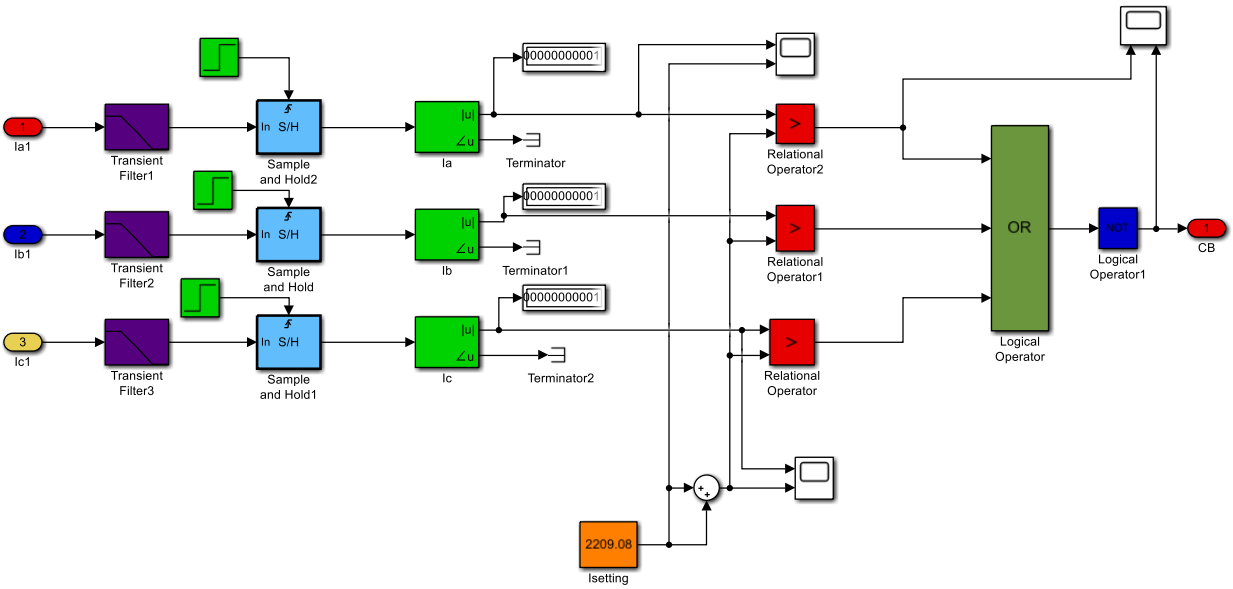

Fig. 6. Overcurrent relay logic model.

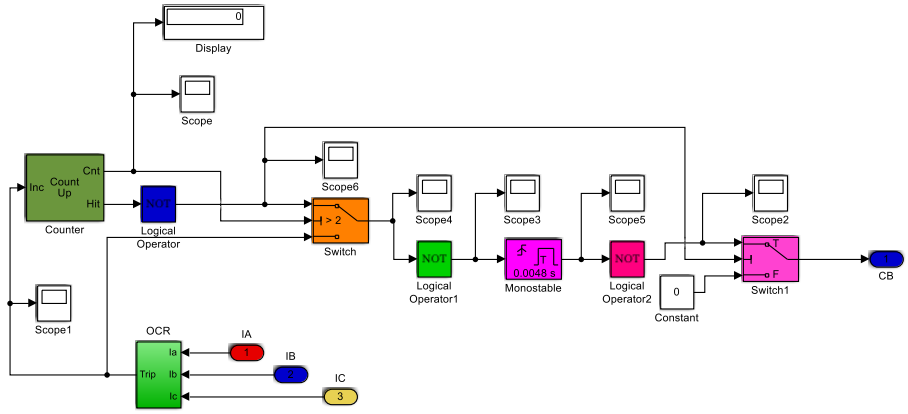

Fig. 7. Auto-Reclose with overcurrent relay logic model.

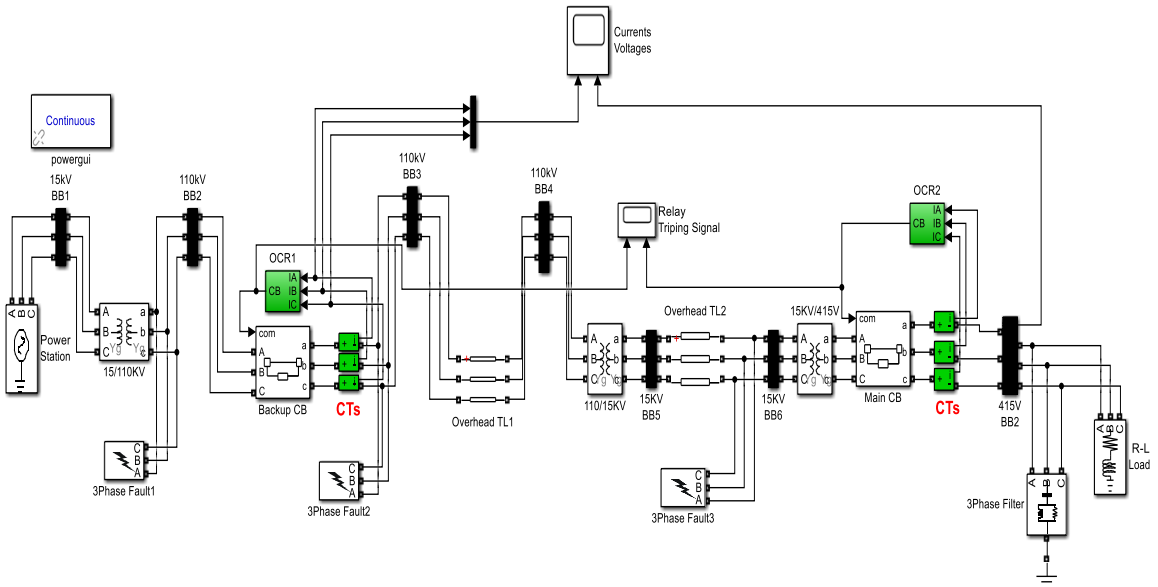

Fig. 8. Electricity grid with overcurrent and auto-reclose relays protection after faults.

ISSN 2096-0042 CN 10-1328/TM

VI. RESULTS AND DISCUSSION

4.1 Overcurrent Relay Settings and Coordination

The corresponding impedances and short circuit currents have been computed using 0%, 1%, 25%, 50%, 75%, and 100% feeder locations from the substation's distribution transformer, respectively.

a) At 0% fault location of the feeder,

The fault point was calculated using the distributed transformer within the substation and the outgoing feeder impedance. Equations (5) and (7) are used to compute the equivalency impedance. Hence, $Z_{eq} = X_t + X_{f15kV} =$ j0.086+j1.95 = j2.036 in Ω

$Z_{1eq} = Z_{2eq} = Z_{eq} =$ j2.036 in Ω/km, real impedance $|Z_{1eq} = Z_{2eq}| = \sqrt[2]{2.036^2} = 2.036\Omega$

The phase-to-phase short circuit currents (I_{SC}) in the feeder was influenced by the positive and negative sequence of equivalent impedance (Z_{1eq} and Z_{2eq}) at every, fault location and fault currents were found as shown in equation (17).

$$I_{SC} = \frac{V_{15KV}}{2Z_{eq}} \quad (17)$$

Where $|Z_{1eq} = Z_{2eq}|$ is the equivalence impedance and V_{15KV} is the phase-to-phase voltage at 15 kV side and Z_{eq} is the equivalence impedance of the power system.

So, $I_{SC} = \frac{15*10^3}{2*2.036} = \mathbf{3683.693A}$

b) At 1% fault location of the feeder,

$Z_{1eq} = Z_{2eq} =$ j2.036 + 0.0026 + j0.088 in Ω/km $=$ $0.026 + j2.124$

$|Z_{1eq} = Z_{2eq}| = \sqrt[2]{0.026^2 + 2.124^2} = 2.124\Omega$

So, $I_{SC} = \frac{15*10^3}{2*2.124} = \mathbf{3531.073A}$

c) At 25% fault location of the feeder,

$Z_{1eq} = Z_{2eq} = 25\% * 58.5 * (0.045 + j0.151) + j2.036 = 0.658 + j4.244$

$|Z_{1eq} = Z_{2eq}| = \sqrt[2]{0.658^2 + 4.244^2} = 4.294\Omega$

So, $I_{SC} = \frac{15*10^3}{2*4.294} = \mathbf{1746.6A}$

d) At 50% fault location of the feeder,

$Z_{1eq} = Z_{2eq} = 50\% * 58.5 * (0.045 + j0.151) + j2.036$

$= 1.316 + j6.452$

$|Z_{1eq} = Z_{2eq}| = \sqrt[2]{1.316^2 + 6.452^2} = 7.207\Omega$, and $I_{SC} = \frac{15*10^3}{2*7.207} = \mathbf{1040.582A}$

e) At 75% fault location of the feeder,

$Z_{1eq} = Z_{2eq} = 75\% * 58.5 * (0.045 + j0.151) + j2.036$

$= 1.974 + j8.661$

$|Z_{1eq} = Z_{2eq}| = \sqrt[2]{1.974^2 + 8.661^2} = 8.883\Omega$

So, $I_{SC} = \frac{15*10^3}{2*8.883} = \mathbf{844.309A}$

f) At 100% fault location of the feeder

$Z_{1eq} = Z_{2eq} = 100\% * 58.5 * (0.045 + j0.151) + j2.036$

$= 2.632 + j10.869$

$|Z_{1eq} = Z_{2eq}| = \sqrt[2]{2.632^2 + 10.869^2} = 11.183\Omega$

So, $I_{SC} = \frac{15*10^3}{2*11.183} = \mathbf{670.66A}$

The maximum fault current level occurred in grid was considered to 13489A. This paper expected to protect the combination of the expected fault currents with the highest fault current that was reached in the protected network at every short circuit current calculated on each fault location. Table 3 shows the fault current levels that were taken into consideration as determined previously during intelligent modeling and simulation of fault power network in this paper.

Table 3. Calculated and estimated fault currents based on maximum fault level.

% Fault locations in the Feeder lines	Calculated Fault level Current (I_{SC}) (A)	Occurred Fault Level (A)	Protected Fault current level ($I_{SC} + I_{Fault-max}$) (A)
0	3683.693	13489.00	17172.693
1	3531.073	11572.35	17020.073
25	1746.6	8574.92	15235.600
50	1040.582	10859.115	14529.582
75	844.309	2238.55	14333.309
100	670.66	5951.29	14159.660

4.2 OCR incoming of the power network

The relay operating times were obtained using the fault positions and relay characteristics.

a) At 0% fault position

$I_{set} = 2209.08$ A and TMS $= 0.05$sec, $I_{sc} = 17172.693$A as shown in equation (16), and table 3

i. Standard inverse relay characteristics

$$t_{OCR} = \frac{0.14}{\left(\frac{I_{sc}}{I_{set}}\right)^{0.02} - 1} * TMS = \frac{0.14}{\left(\frac{17172.693}{2209.08}\right)^{0.02} - 1} * 0.05 = \mathbf{0.167sec}$$

ii. Very Inverse relay characteristics

$$t_{OCR} = \frac{13.5}{\left(\frac{I_{sc}}{I_{set}}\right) - 1} * TMS = \frac{13.5}{\left(\frac{17172.693}{2209.08}\right) - 1} * 0.05 = \mathbf{0.096sec}$$

iii. Extremely Inverse relay characteristics

$$t_{OCR} = \frac{80}{\left(\frac{I_{sc}}{I_{set}}\right)^2 - 1} * TMS = \frac{80}{\left(\frac{17172.693}{2209.08}\right)^2 - 1} * 0.05 = \mathbf{0.067sec}$$

b) At 1% fault position

$I_{set} = 2209.08$ A and TMS $= 0.05$ sec, $I_{sc} = 17020.073$A , as shown in equation (16), and Table 3.

i. Standard Inverse relay characteristics

$$t_{OCR} = \frac{0.14}{(\frac{I_{sc}}{I_{set}})^{0.02} - 1} * TMS = \frac{0.14}{\left(\frac{17020.073}{2209.08}\right)^{0.02} - 1} * 0.05$$
$$= \mathbf{0.168sec}$$

ii. Very Inverse relay characteristics

$$t_{OCR} = \frac{13.5}{(\frac{I_{sc}}{I_{set}}) - 1} * TMS = \frac{13.5}{\left(\frac{17020.073}{2209.08}\right) - 1} * 0.05$$
$$= \mathbf{0.100sec}$$

iii. Extremely Inverse relay characteristics

$$t_{OCR} = \frac{80}{(\frac{I_{sc}}{I_{set}})^2 - 1} * TMS = \frac{80}{\left(\frac{17020.073}{2209.08}\right)^2 - 1} * 0.05$$
$$= \mathbf{0.0685sec}$$

c) At 25% fault position.

$I_{set} = 2209.08$ A and $TMS = 0.05$ sec, $I_{sc} = 15235.600$A, as shown in equation (16), and table 3,

i. Standard Inverse relay characteristics

$$t_{OCR} = \frac{0.14}{(\frac{I_{sc}}{I_{set}})^{0.02} - 1} * TMS = \frac{0.14}{\left(\frac{15235.6}{2209.08}\right)^{0.02} - 1} * 0.05$$
$$= \mathbf{0.178sec}$$

ii. Very Inverse relay characteristics

$$t_{OCR} = \frac{13.5}{(\frac{I_{sc}}{I_{set}}) - 1} * TMS = \frac{13.5}{\left(\frac{15235.6}{2209.08}\right) - 1} * 0.05$$
$$= \mathbf{0.1144sec}$$

iii. Extremely Inverse relay characteristics

$$t_{OCR} = \frac{80}{(\frac{I_{sc}}{I_{set}})^2 - 1} * TMS = \frac{80}{\left(\frac{15235.6}{2209.08}\right)^2 - 1} * 0.05$$
$$= \mathbf{0.085sec}$$

d) At 50% fault position.

$I_{set} = 2209.08$ A and $TMS = 0.05$ sec, $I_{sc} = 14529.582$A , as shown in equation (16), and table 3,

i. Standard Inverse relay characteristics

$$t_{OCR} = \frac{0.14}{\left(\frac{I_{sc}}{I_{set}}\right)^{0.02} - 1} * TMS = \frac{0.14}{\left(\frac{14529.582}{2209.08}\right)^{0.02} - 1} * 0.05$$
$$= \mathbf{0.182sec}$$

ii. Very Inverse relay characteristics

$$t_{OCR} = \frac{13.5}{(\frac{I_{sc}}{I_{set}}) - 1} * TMS = \frac{13.5}{\left(\frac{14529.582}{2209.08}\right) - 1} * 0.05$$
$$= \mathbf{0.121sec}$$

iii. Extremely Inverse relay characteristics

$$t_{OCR} = \frac{80}{(\frac{I_{sc}}{I_{set}})^2 - 1} * TMS = \frac{80}{\left(\frac{14529.582}{2209.08}\right)^2 - 1} * 0.05$$
$$= \mathbf{0.0946sec}$$

a) At 75% fault position

$I_{set} = 2209.08$ A and $TMS = 0.05$ sec, $I_{sc} = 14333.309$A, as shown in equation (16), and table 3.

i. Standard Inverse relay characteristics

$$t_{OCR} = \frac{0.14}{(\frac{I_{sc}}{I_{set}})^{0.02} - 1} * TMS = \frac{0.14}{\left(\frac{14333.309}{2209.08}\right)^{0.02} - 1} * 0.05$$
$$= \mathbf{0.1836sec}$$

ii. Very Inverse relay characteristics

$$t_{OCR} = \frac{13.5}{(\frac{I_{sc}}{I_{set}}) - 1} * TMS = \frac{13.5}{\left(\frac{14333.309}{2209.08}\right) - 1} * 0.05$$
$$= \mathbf{0.122sec}$$

iii. Extremely Inverse relay characteristics

$$t_{OCR} = \frac{80}{(\frac{I_{sc}}{I_{set}})^2 - 1} * TMS = \frac{80}{\left(\frac{14333.309}{2209.08}\right)^2 - 1} * 0.05$$
$$= \mathbf{0.0973sec}$$

a) At 100% fault position

$I_{set} = 2209.08$ A and $TMS = 0.05$ sec, $I_{sc} = 14159.66$A, as shown in equation (16), and table 3,

i. Standard Inverse relay characteristics

$$t_{OCR} = \frac{0.14}{(\frac{I_{sc}}{I_{set}})^{0.02} - 1} * TMS = \frac{0.14}{\left(\frac{14159.66}{2209.08}\right)^{0.02} - 1} * 0.05$$
$$= \mathbf{0.184sec}$$

ii. Very Inverse relay characteristics

$$t_{OCR} = \frac{13.5}{(\frac{I_{sc}}{I_{set}}) - 1} * TMS = \frac{13.5}{\left(\frac{14159.66}{2209.08}\right) - 1} * 0.05$$
$$= \mathbf{0.1247sec}$$

iii. Extremely Inverse relay characteristics

$$t_{OCR} = \frac{80}{(\frac{I_{sc}}{I_{set}})^2 - 1} * TMS = \frac{80}{\left(\frac{14159.66}{2209.08}\right)^2 - 1} * 0.05$$
$$= \mathbf{0.0998sec}$$

4.3 OCR Outgoing of the feeder

a) At 0% fault position

$I_{set} = 600A$ and $TMS = 0.05$ sec, $I_{sc} = 17172.693A$ as shown in equation (15), and table 3,

i. Standard inverse relay characteristics

$$t_{OCR} = \frac{0.14}{(\frac{I_{sc}}{I_{set}})^{0.02} - 1} * TMS = \frac{0.14}{\left(\frac{17172.693}{600}\right)^{0.02} - 1} * 0.05$$
$$= \mathbf{0.1008sec}$$

ii. Very Inverse relay characteristics

$$t_{OCR} = \frac{13.5}{(\frac{I_{sc}}{I_{set}}) - 1} * TMS = \frac{13.5}{\left(\frac{17172.693}{600}\right) - 1} * 0.05$$
$$= \mathbf{0.024sec}$$

iii. Extremely Inverse relay characteristics

$$t_{OCR} = \frac{80}{(\frac{I_{sc}}{I_{set}})^2 - 1} * TMS = \frac{80}{\left(\frac{17172.693}{600}\right)^2 - 1} * 0.05$$
$$= \mathbf{0.0048sec}$$

b) At 1% fault position

$I_{set} = 600$ A and $TMS = 0.05$ sec, $I_{sc} = 17020.073$ A as shown in equation (15), and table 3,

i. Standard Inverse relay characteristics

$$t_{OCR} = \frac{0.14}{(\frac{I_{sc}}{I_{set}})^{0.02} - 1} * TMS = \frac{0.14}{\left(\frac{17020.073}{600}\right)^{0.02} - 1} * 0.05$$
$$= \mathbf{0.101sec}$$

ii. Very Inverse relay characteristics

$$t_{OCR} = \frac{13.5}{(\frac{I_{sc}}{I_{set}}) - 1} * TMS = \frac{13.5}{\left(\frac{17020.073}{600}\right) - 1} * 0.05$$
$$= \mathbf{0.0246sec}$$

iii. Extremely Inverse relay characteristics

$$t_{OCR} = \frac{80}{(\frac{I_{sc}}{I_{set}})^2 - 1} * TMS = \frac{80}{\left(\frac{17020.073}{600}\right)^2 - 1} * 0.05$$
$$= \mathbf{0.00497sec}$$

c) At 25% fault position

$I_{set} = 600$ A and $TMS = 0.05$ sec, $I_{sc} = 15235.60$, as shown in equation (15) and Table 3.

i. Standard Inverse relay characteristics

$$t_{OCR} = \frac{0.14}{(\frac{I_{sc}}{I_{set}})^{0.02} - 1} * TMS = \frac{0.14}{\left(\frac{15235.6}{600}\right)^{0.02} - 1} * 0.05$$
$$= \mathbf{0.104sec}$$

ii. Very Inverse relay characteristics

$$t_{OCR} = \frac{13.5}{(\frac{I_{sc}}{I_{set}}) - 1} * TMS = \frac{13.5}{\left(\frac{15235.6}{600}\right) - 1} * 0.05$$
$$= \mathbf{0.0276sec}$$

iii. Extremely Inverse relay characteristics

$$t_{OCR} = \frac{80}{(\frac{I_{sc}}{I_{set}})^2 - 1} * TMS = \frac{80}{\left(\frac{15235.6}{600}\right)^2 - 1} * 0.05$$
$$= \mathbf{0.00621sec}$$

d) At 50% fault position

$I_{set} = 600$ A and $TMS = 0.05$, $I_{sc} = 14529.582A$, as shown in equation (15) and table 3,

i. Standard Inverse relay characteristics

$$t_{OCR} = \frac{0.14}{(\frac{I_{sc}}{I_{set}})^{0.02} - 1} * TMS = \frac{0.14}{\left(\frac{14529.582}{600}\right)^{0.02} - 1} * 0.05$$
$$= \mathbf{0.1063sec}$$

ii. Very Inverse relay characteristics

$$t_{OCR} = \frac{13.5}{(\frac{I_{sc}}{I_{set}}) - 1} * TMS = \frac{13.5}{\left(\frac{14529.582}{600}\right) - 1} * 0.05$$
$$= \mathbf{0.029sec}$$

iii. Extremely Inverse relay characteristics

$$t_{OCR} = \frac{80}{(\frac{I_{sc}}{I_{set}})^2 - 1} * TMS = \frac{80}{\left(\frac{14529.582}{600}\right)^2 - 1} * 0.05$$
$$= \mathbf{0.00683sec}$$

e) At 75% fault position

$I_{set} = 600$ A and $TMS = 0.05$ sec, $I_{sc} = 14333.309$A , as shown in equation (15), and table 3.

i. Standard Inverse relay characteristics

$$t_{OCR} = \frac{0.14}{(\frac{I_{sc}}{I_{set}})^{0.02} - 1} * TMS = \frac{0.14}{\left(\frac{14333.309}{600}\right)^{0.02} - 1} * 0.05$$
$$= \mathbf{0.1068sec}$$

ii. Very Inverse relay characteristics

$$t_{OCR} = \frac{13.5}{\left(\frac{I_{sc}}{I_{set}}\right) - 1} * TMS = \frac{13.5}{\left(\frac{14333.309}{600}\right) - 1} * 0.05$$
$$= \mathbf{0.0294sec}$$

iii. Extremely Inverse relay characteristics

$$t_{OCR} = \frac{80}{(\frac{I_{sc}}{I_{set}})^2 - 1} * TMS = \frac{80}{\left(\frac{14333.309}{600}\right)^2 - 1} * 0.05$$
$$= \mathbf{0.00702sec}$$

f) At 100% fault position

$I_{set} = 600$ A and $TMS = 0.05$ sec, $I_{sc} = 14159.6$, as shown in equation (15), and Table 3.

i. Standard Inverse relay characteristics

$$t_{OCR} = \frac{0.14}{(\frac{I_{sc}}{I_{set}})^{0.02} - 1} * TMS = \frac{0.14}{\left(\frac{14159.66}{600}\right)^{0.02} - 1} * 0.05$$
$$= \mathbf{0.10725sec}$$

ii. Very Inverse relay characteristics

$$t_{OCR} = \frac{13.5}{(\frac{I_{sc}}{I_{set}}) - 1} * TMS = \frac{13.5}{\left(\frac{14159.66}{600}\right) - 1} * 0.05$$
$$= \mathbf{0.0298sec}$$

iii. Extremely Inverse relay characteristics

$$t_{OCR} = \frac{80}{(\frac{I_{sc}}{I_{set}})^2 - 1} * TMS = \frac{80}{\left(\frac{14159.66}{600}\right)^2 - 1} * 0.05$$
$$= \mathbf{0.00719sec}$$

Table 4 tabulates and summarizes the operating and coordination times of overcurrent relay characteristics acquired. Based on the standard, very, and extremely inverted overcurrent relay characteristics, the OCR fault clearing and coordination times are 98.97% faster than the distance relay protections and other evaluated protection schemes during fault occurrence in the Rwanda power network. By taking into account the OCR characteristics, the OCR performance with regard to fault current sites and fault clearing periods based on OCR incoming and outgoing (feeders) was observed and is shown in Fig. 9. The relaying system's coordination time was calculated using the interval period between incoming and outgoing (feeders) with OCR characteristics in mind.

Table 4. The results of the time of incoming and outgoing feeders for Extremely Inverse, Very Inverse, and Standard Inverse Relay Characteristics of the Overcurrent Relay

Fault Positions (%)	Operating Time (Sec)						Coordination Time Interval(Δt) in sec		
	OCR INCOMING			OCR OUTGOING			$t_{incoming} - t_{outgoing}$		
	EI	VI	SI	EI	VI	SI	EI	VI	SI
0	0.067000	0.096000	0.167000	0.004800	0.024000	0.100900	0.062200	0.072000	0.066100
1	0.068500	0.100000	0.168000	0.004900	0.024600	0.101100	0.063600	0.075400	0.066900
25	0.085000	0.114400	0.178000	0.006200	0.027600	0.104500	0.07800	0.086800	0.073500
50	0.094600	0.121000	0.182000	0.006800	0.029000	0.106400	0.087800	0.092000	0.075600
75	0.097300	0.122000	0.183000	0.007000	0.029400	0.107200	0.090300	0.092600	0.075800
100	0.099800	0.124700	0.184000	0.007100	0.029800	0.107600	0.092700	0.094900	0.076400

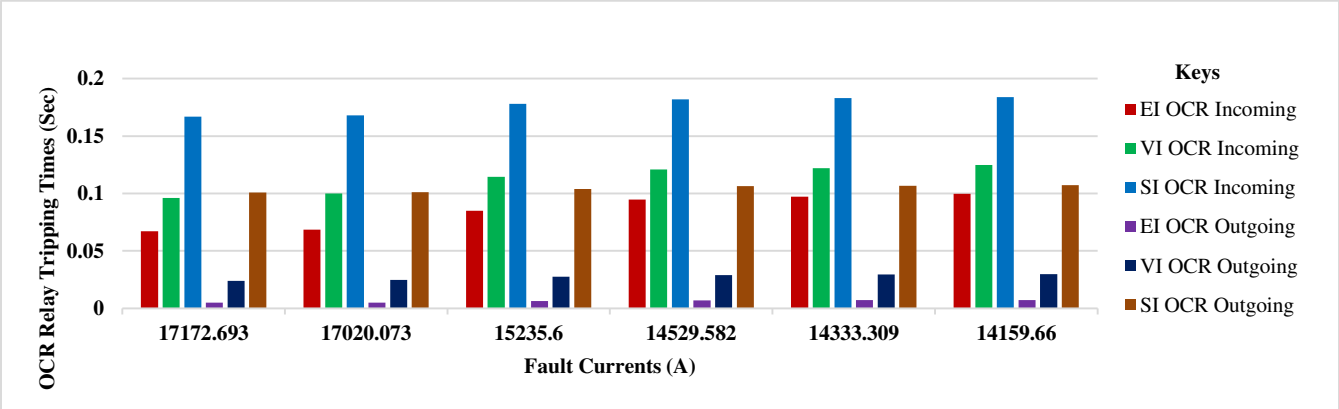

Fig. 9. The operating times of OCR characteristics of incoming and outgoing observances.

The simulation results of tripping signals of overcurrent relays, current, and voltage signals before, during, and after fault conditions in this research were demonstrated and performed using MATLAB/Simulink 2019a package as shown in Fig. 10 and Fig. 11, respectively.

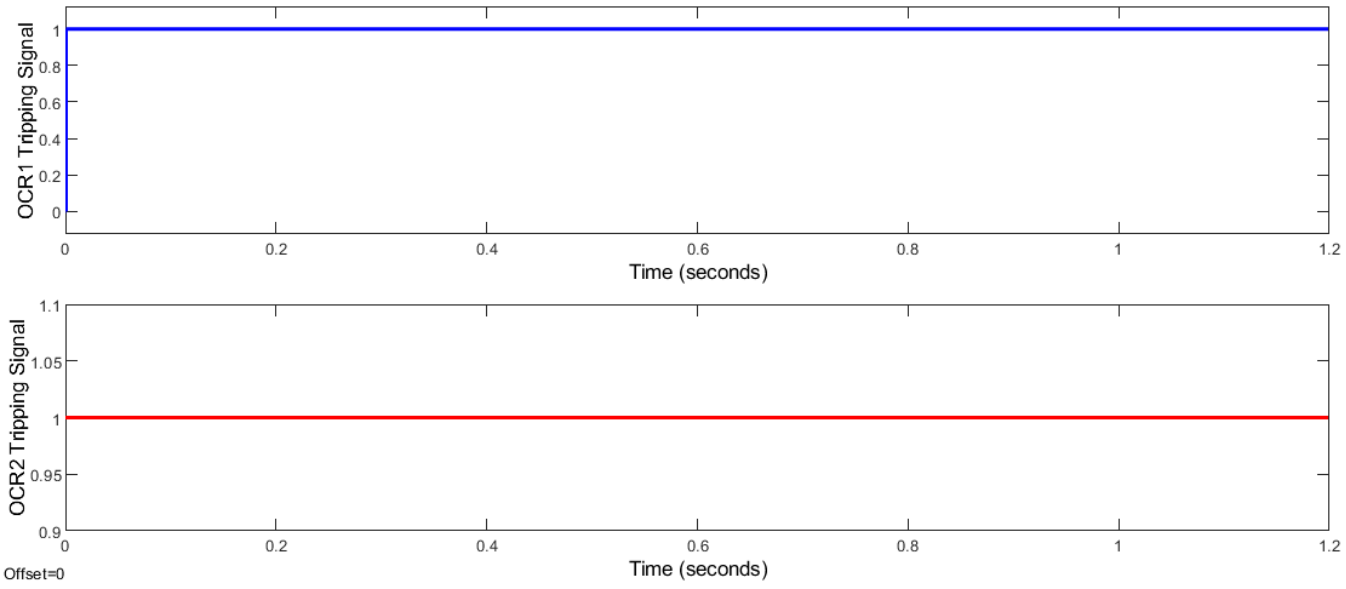

Fig. 10. Power network relay tripping signals at their operational states.

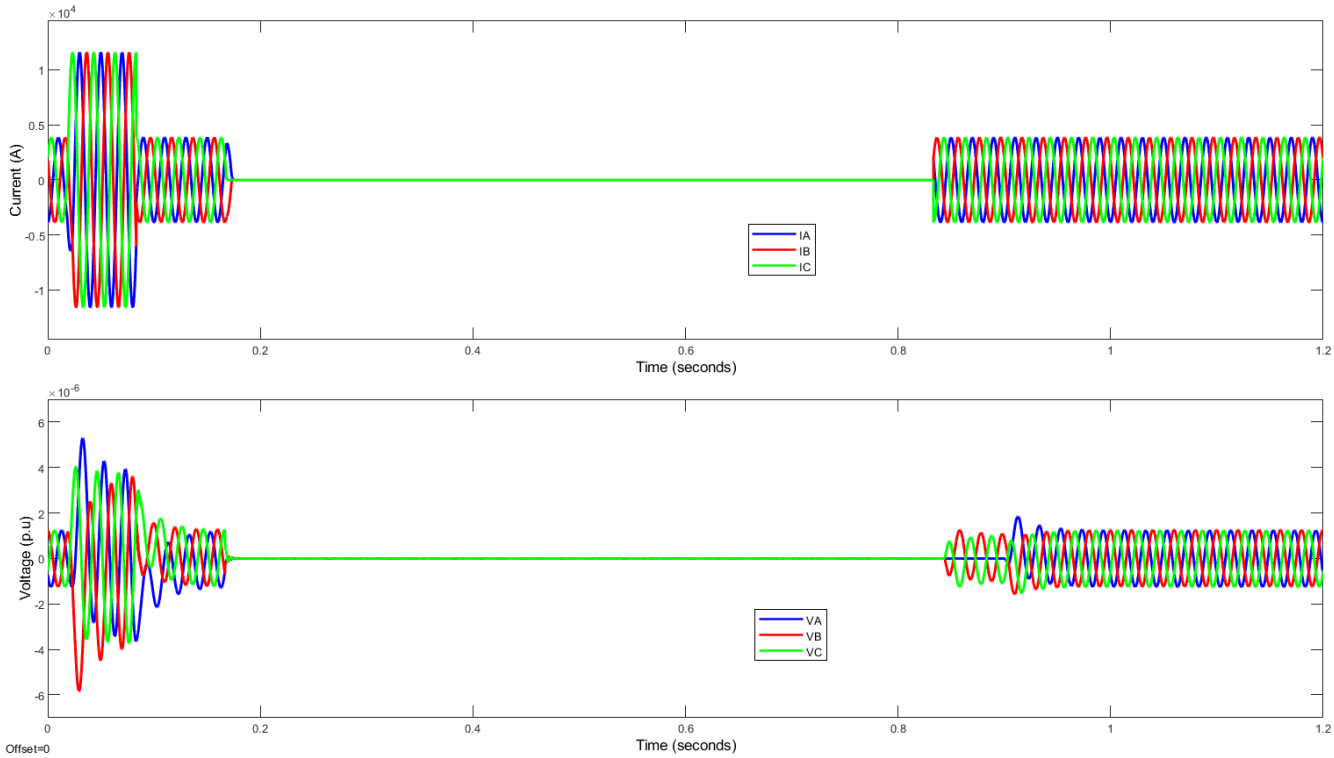

Fig. 11. Voltages and Currents were observed at normal, faulty conditions, and fault clearance during a simulation of the power system.

Their qualities, which revealed how fast they performed, largely affected relay coordination and settings. It included Standard Inverse, Very Inverse, and Extremely Inverse. As demonstrated in Fig. 9 and Table 4, the extremely inverse, very inverse, and standard inverse of the overcurrent relay were conducted between 0.0927 sec - 0.062 sec, 0.0949 sec - 0.0720 sec, and 0.0764 sec - 0.0661 sec for overcurrent incoming and outgoing feeders, respectively. Based on the short circuit currents listed in Table 3, the operating time of overcurrent incoming and outgoing feeders was calculated, and the time setting multiplier was set at 0.05seconds (IEC standards). In this study, it was demonstrated that by operating overcurrent relays and creating three-phase faults in the network on the power station and transmission line sides, or at any location in the power electricity network, there was an improvement and optimization of 99.98% rate of OCR performance during fault occurrence and clearing periods compared to the distance relay protection scheme. The voltage and current waveforms observed during transmission line simulations before, during, and after fault circumstances, as well as after power outages, were cleared in 0.06 seconds, demonstrating how quick the OCR settings established in this research are. Figure 8 depicts the creation of three-phase faults and the modeling of the power network system. The OCR 1 and OCR 2 were coordinated and sent the tripping signals to Backup CB and Main CB, respectively. The relay system successfully isolated a faulted power grid part and tripped the network within 0.01 seconds. The fault current was high at 0.039 seconds, and the faults remained in the network for 0.6 seconds. The voltage decreased to zero volts instantly, but was cleared by OCR relays. The faulted part was quickly restored in 0.7 seconds. The cascade power outage events were caused by lightning surges and distribution transformer overload. The auto-reclose relay checked the synchronism of interconnected networks to prevent power blackouts. The faults occurred at 0.016 seconds and caused voltage fluctuations. The faults resisted and cleared within 0.066 seconds, and the network was restored within 0.17 seconds. The OCR operation times varied, with highly inverse relays taking the shortest time.

V. CONCLUSION AND FUTURE WORKS

The study analyzed the operation and coordination of OCR settings, considering three OCR characteristics: extremely inverse, very inverse, and standard inverse. The relays were operated in 0.0328 seconds for OCR incoming and 0.0023 seconds for OCR outgoing (feeders). The OCR settings and substation coordination were actuated in 0.0103 seconds, 0.0229 seconds, and 0.0305 seconds for the overcurrent relays. The standard inverse of the relay was recommended for the HV utility substation. The very inverse was used in the midpoint of feeders, while the extremely inverse cleared faults at the far end. The paper also considered phase-to-phase faults and OCR relay types for their reliability, fastness, and accurate observations. Future studies should include induction type relays, frequency monitoring relays, zone impedance relays, direction relays, and other types of relays. Real-time simulation software with artificial intelligence coordination is highly recommended for cybersecurity issues.

Data Availability

The research covers all of the needed data. More data is available upon request from the main author.

Conflict of interest

No conflicting of interests.

ACKNOWLEDGMENT

The authors express gratitude to Moi University for providing laboratory facilities for their research, which was funded by the World Bank through the African Center of Excellence in Phytochemical, Textile, and Renewable Energy (ACE II PTRE).

REFERENCES

[1] Syed Norazizul SYED NASIR, Abdullah Asuhaimi MOHD ZIN, "Instantaneous protection scheme for backup protection of high-voltage transmission lines," Turkish Journal of Electrical Engineering & Computer Sciences, vol. 25, no. 7, p. 3261 – 3272, 2023.

[2] G. Multilin Electric, Line Protection with Overcurrent Relays, Paris, France: General Electric, https://www.gegridsolutions.com/, 2023.

[3] T. Holmes, Protection of Electricity Distribution Networks, 2nd Edition, Setting Overcurrent Relays, Washington, USA: GlobalSpec, 2023.

[4] H. Amreiz, A. Janbey, M. Darwish, "Emulations of Overvoltage and Overcurrent Relays In Transmission Lines," in 2022 57th International Universities Power Engineering Conference (UPEC), London, UK, 2022.

[5] R. Mohammadi, "Optimal Relays Coordination Efficient method in Interconnected Power Systems," Journal of electrical engineering (JEE), vol. LXI, no. 2, pp. 75-83, 2010.

[6] NEPA., Basic Protection Course P1''Training and development program., Washington: NEPA., 2007.

[7] Goh H. H., Chua Q. S., Lee S. W., Kok B. C., Goh K. C., Comparative Study of Line Voltage Stability Indices for Voltage Collapse Forecasting in Power Transmission System., Rio de Janeiro, Brazil: Chua, Q. S, 2015.

[8] Mininfra, "Energy transmission voltage levels in Rwanda," Mininfra, Kigali, 2018.

[9] Sachdev M., "Advancements in microprocessor-based protection," IEEE Tutorial Coerce Text, Publication No 97TP120-0, vol. II, no. 15, pp. 120-121, 2015.

[10] Suryanarayana Gangolu, Saumendra Sarangi, "A novel complex current ratio-based technique for transmission line protection," Springer, Protection and Control of Modern Power Systems, vol. 15, no. 23, pp. 1750-1765, 2020.

[11] Zhaohui Chen, Xiaobing Ding, Mingjun Xue, Hao Zhang, "Relay Protection Method of High Voltage Transmission Line Based on Time-frequency Analysis," Journal of Physics, 2022 International Conference on Energy and Power Engineering (EPE 2022), http://dx.doi.org/10.1088/1742-6596/2442/1/012032, vol. 2442, no. 1, pp. 1-8, 2023.

[12] Hao Kong, Wei Cong, Hongzhe Zhang, Jifu Qiu, Ming Chen, Zhen Wei, "New Protection Method for High-Voltage Transmission Lines Based on Traveling Wave Energy Comparison," 2021 IEEE/IAS Industrial and Commercial Power System Asia (I&CPS Asia), Chengdu, China, 2021.

[13] Sauvik Biswas, Paresh Kumar Nayak, Bijaya Ketan Panigrahi, "Protection of High Voltage Transmission Lines Connected to Large-Scale Wind Farms: A Review," in Power Quality: Infrastructures and Control, Studies in Infrastructure and Control , Singapore, Springer, https://link.springer.com/chapter/10.1007/978-981-19-7956-9_13, 2023.

[14] D. Kostić, "documentation/typhoon-hil-application-notes/References," 04 August 2021. [Online]. Available: https://www.typhoon-hil.com.

[15] Wang J., Jiping Lu, Hongji Xiang, Xing Ma, Hui Fang., "Distance protection of EHV long transmission lines considering compensation degree of shunt reactor," Global Energy Interconnection Development and Cooperation Organization by Elsevier B.V, pp. 64-70, 2019.

[16] J. McConnell A., Complete Your Back-Up Protection of Transmission Lines/Line Protection with distance relays, Electric World, 1952.

BIOGRAPHY

Boniface NTAMBARA, born in Rwanda in 1992, holds a BSc (Eng.) degree in Electrical Power Engineering from the University of Rwanda/College of Science and Technology, Rwanda, in 2015; MSc in Industrial Engineering from Moi University, Kenya, in 2022 and MSc in Embedded and Mobile Systems (Embedded System Option) from Nelson Mandela African Institution of Science and Technology, Tanzania in 2023.

Paul M. Wambua is a full professor-engineer of materials engineering from Moi University. He received BSc in textile engineering from University of Engineering and Technology Lahore (Pakistan) in 1989, MSc in Textile Science and Engineering from the University of Leeds (United Kingdom) in 1995, Doctor of Engineering from Katholieke Universiteit Leuven (Belgium). He is currently Deputy Vice-chancellor, Institutional Advancement and Enterprise (IAE), in the Technical University of Kenya.

Jean Bosco Byiringiro is professor-engineer of mechatronics and automation engineering from Dedan Kimathi University of Technology in Kenya. He received BSc in Electro-Mechanical Engineering from Kigali Institute of Science and Technology-Rwanda in 2005, MSc in Mechatronic Engineering from Jomo Kenyatta university of Agriculture and Technology, Kenya in 2009, PhD in Mechanical Engineering in the area of Micro/Nano Fabrication from Yeungnam University, South Korea in 2012.

Simiyu Stanley Sitati is a Professor-Engineer of Electrical and Telecommunication Engineering from Moi University. He received PhD in Electrical Engineering from Moscow Power Engineering Institute-Technical University in 2000.

ISSN 2096-0042 CN 10-1328/TM